Microcapsule induced toughening in a self-healing polymer composite*

E. N. BROWN[1,2], S. R. WHITE[3,2], and N. R. SOTTOS[1,2]

[1]Department of Theoretical and Applied Mechanics
University of Illinois at Urbana-Champaign, Urbana, IL, 61801
[2]Beckman Institute for Advanced Science and Technology
University of Illinois at Urbana-Champaign, Urbana, IL, 61801
[3]Department of Aeronautical & Astronautical Engineering
University of Illinois at Urbana-Champaign, Urbana, IL, 61801

Abstract

Microencapsulated dicyclopentadiene (DCPD) healing agent and Grubbs' Ru catalyst are incorporated into an epoxy matrix to produce a polymer composite capable of self-healing. The fracture toughness and healing efficiency of this composite are measured using a tapered double-cantilever beam (TDCB) specimen. Both the virgin and healed fracture toughness depend strongly on the size and concentration of microcapsules added to the epoxy. Fracture of the neat epoxy is brittle, exhibiting a mirror fracture surface. Addition of DCPD-filled urea-formaldehyde (UF) microcapsules yields up to 127% increase in fracture toughness and induces a change in the fracture plane morphology to hackle markings. The fracture toughness of epoxy with embedded microcapsules is much greater than epoxy samples with similar concentrations of silica microspheres or solid UF polymer particles. The increased toughening associated with fluid-filled microcapsules is attributed to increased hackle markings as well as subsurface microcracking not observed for solid particle fillers.

1. Introduction

A novel approach to recover the fracture properties of thermosetting polymers has been introduced by White *et al.* [1]. Healing is achieved by incorporating a microencapsulated healing agent and a catalytic chemical trigger within a polymer matrix. A propagating crack ruptures the microcapsules and exposes catalyst particles. Crack opening draws the healing agent into the crack plane, where contact with the catalyst phase initiates polymerization. The polymerized healing agent reestablishes structural integrity across the crack plane.

Conclusive demonstration of self-healing was obtained with a healing agent based on the ring-opening metathesis polymerization (ROMP) reaction [1]. Dicyclopentadiene (DCPD), a highly stable monomer with excellent shelf life, was encapsulated in urea-formaldehyde (UF) microcapsules. A small volume fraction of microcapsules was dispersed in an epoxy matrix along with Grubbs' transition metal catalyst [2]. This self-healing epoxy was able to recover over 90% of its virgin fracture toughness [3]. In addition to providing an efficient mechanism for self-healing, the presence of DCPD-filled UF microcapsules also significantly increased the inherent fracture toughness of the epoxy.

In the present work, we investigate toughening mechanisms induced by embedded microcapsules in a self-healing epoxy and the corresponding effect on healing efficiency. Several investigations of microcapsule-filled polymers have appeared in the literature using alternate terms such as hollow spheres [4], cenospheres [5], microballons [6,7], hollow particles [8,9], hollow microspheres [8,10], and bubbles [11]. Most of the literature examines the behavior of glass (rather than polymer) microcapsules, with mixed conclusions regarding the effect on fracture behavior. Azimi *et al*. [4] found a 126% increase in fracture toughness for epoxy (DGEBA cured with piperadine) with the addition of 10 vol% of glass microcapsules. Similarly, a 185% increase in toughness was measured for polyester filled with 27 vol% silane coated glass microcapsules [5]. In contrast, Zihlif and Ragosta [6] reported a 33% reduction of toughness under impact loading with the addition of 10 vol% glass microcapsules in epoxy (DGEBA cured with a polyamide). El-Hadek and Tippur [7] also found a 20% reduction of toughness for epoxy and urethane filled with 10 vol% glass microcapsules. Fewer investigations of polymer microcapsules have appeared in the literature, but all have consistently reported increases in fracture toughness. Begheri and Pearson [8] added latex and acrylic microcapsules to epoxy (DGEBA cured with aminoethyl piperazine) and found fracture toughness increased by 141% for 10 vol% microcapsules. Toughening by sub 15 μm diameter microcapsules was attributed to shear yielding at the crack tip, while a combination of shear yielding and microcracking was identified as the operative mechanism at larger

diameters. Jung [12] also measured significant toughening with the addition of epoxide-filled polyoxymethylene urea (PMU) microcapsules to a DCPD polyester matrix.

Although the mechanisms are not well understood, results of these previous investigations combined with recent observations in self-healing polymers indicate that polymer microcapsules significantly toughen a brittle polymer matrix. In the current work, we seek to elucidate the specific toughening mechanisms associated with the addition of polymer microcapsules through extensive fracture testing, examination of fracture surfaces and comparison with other types of particle reinforcement.

2. Experimental procedure

2.1. Fracture tests and fractography

The fracture behavior of microcapsule-filled epoxy was investigated using a tapered double-cantilever beam (TDCB) test. Side grooves ensured controlled crack growth along the centerline of the brittle specimen. The TDCB fracture geometry, developed by Mostovoy *et al.* [13], provided a crack-length-independent measure of fracture toughness,

$$K_{IC} = \alpha P_C, \tag{1}$$

which only required measurement of the critical fracture load P_C and knowledge of the geometric term α. For the TDCB sample geometry in Fig. 1, $\alpha = 11.2 \times 10^3$ m$^{-3/2}$ was determined experimentally as discussed by Brown *et al.* [3].

Healing efficiency was assessed using the protocol established by White *et al.* [1]. TDCB fracture specimens were pin loaded and tested under displacement control, at 5 μm/s displacement rate. Samples were tested to failure, measuring compliance and peak load to establish the initial (virgin) fracture toughness. Load was then removed while allowing the crack faces to come back in contact. Samples were retested after 24 hours to
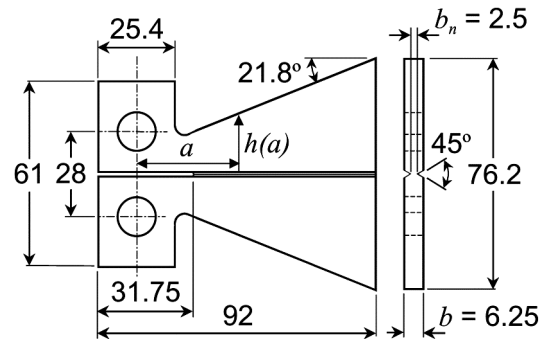

Figure 1 Taper double-cantilever beam (TDCB) geometry [4]. Note: all dimensions in mm.

determine the healed fracture toughness. Crack healing efficiency, η, was defined as the ability to recover fracture toughness [14]. For the TDCB geometry, the healing efficiency was calculated simply as the ratio of critical fracture loads for the healed and virgin samples,

$$\eta = \frac{K_{IC_{healed}}}{K_{IC_{virgin}}} = \frac{P_{C_{healed}}}{P_{C_{virgin}}}. \tag{2}$$

Fracture surface morphologies were examined with a Philips XL30 ESEM-FEG. After fracture, specimens were mounted and sputtered with gold/palladium. Micrographs were obtained using 10kV secondary electrons in high vacuum mode. Cross sections of the fracture plane and subsurface features were further examined by a cryofracture technique [15]. Samples were immersed in liquid nitrogen for approximately one hour, then immediately fractured with a razor blade perpendicular to the original fracture plane and viewed in the ESEM.

2.2. Materials and sample preparation

Urea-formaldehyde microcapsules containing DCPD monomer (Fig. 2) were manufactured with average diameters of 50, 180, and 460 μm using the emulsion *in situ* polymerization microencapsulation method outlined by Brown *et al* [16]. Shell wall thickness was 190 ± 30 nm for all batches. Tapered double-cantilever beam specimens were cast from EPON® 828 epoxy resin (DGEBA) and 12 pph Ancamine® DETA (diethylenetriamine) curing agent with a prescribed concentration of microcapsules and 2.5 wt% catalyst (for self-healing samples) mixed into the resin. The epoxy mixture was degassed, poured into a closed silicone rubber mold and cured for 24 hours at room
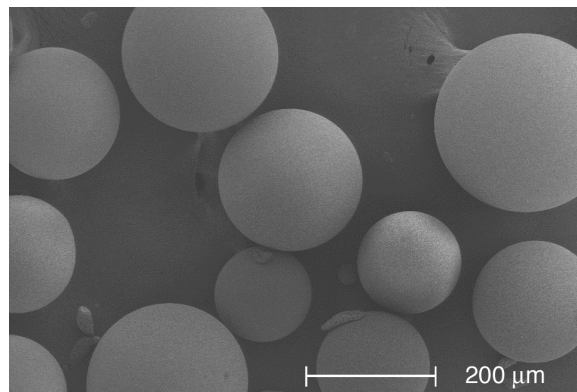

200 μm

Figure 2 Urea-formaldehyde microcapsules containing DCPD prepared by emulsion *in situ* microencapsulation [16].

TABLE 1 Properties of the constituents

Properties	Epoxy	Urea-formaldehyde microcapsules	Silica microspheres
Density (g/cc)	1.16	~1.0	2.51
Diameter (μm)	—	53±19 183±43 458±76	70±12
Wall thickness (nm)	—	190±30	—
K_{Ic} (MPa m$^{1/2}$)	0.55±0.04	—	—
Tensile modulus (GPa)	3.4±0.1	—	—
Tensile strength (MPa)	35±10	—	—

temperature, followed by 24 hours at 30° C. A razor blade was gently tapped into a molded starter notch to generate a sharp precrack. Relevant physical and mechanical properties are listed in Table 1.

Other types of epoxy TDCB samples were also fabricated for comparison of fracture mechanisms. Two different types of solid fillers, silica microspheres and UF particles, and two types of "voids" were investigated. Solid silica microspheres (McMaster-Carr) of ~70 μm average diameter were washed in acetone and baked at 100° C prior to their use in epoxy. For some sample batches the microspheres were treated with a coupling agent (1 pph of Dow z-6040 silane added to the resin) to improve adhesion. UF particles approximately 180 μm in diameter were created by repetitive deposition during emulsion *in situ* polymerization and added to epoxy samples. Voids were introduced into another batch of samples by aggressive mixing of the resin before filling the mold. Samples with poorly bonded microcapsules were obtained by coating UF microcapsules with release agent (Buehler 20-8185-016 and Miller Stephenson MS-122DF).

3. Fracture and self-healing behavior

Virgin fracture toughness is plotted in Fig. 3 as a function of microcapsule concentration for three different microcapsule diameters. Fracture toughness increases with microcapsule concentration until reaching a roughly equivalent peak value for all three capsule sizes. As the microcapsule concentration increases further, the fracture toughness decreases. The average maximum toughness is 127% greater than for neat epoxy (0% microcapsules). The concentration of microcapsules at which the maximum value occurs depends strongly on microcapsule diameter. Smaller microcapsules exhibit maximum toughening at lower concentration.

The healed fracture toughness and healing efficiency are plotted in Fig. 4 for the 50 and 180 μm diameter microcapsule specimens. Healed fracture toughness (Fig. 4a) increases steadily with microcapsule concentration until reaching a plateau at about 20
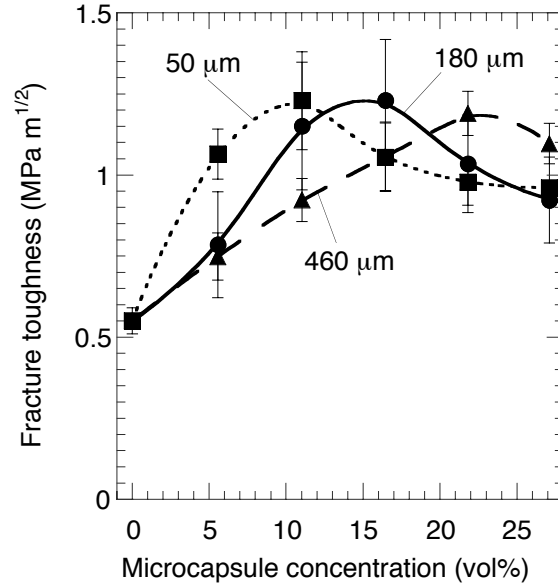
Figure 3 Influence of microcapsule concentration and diameter on fracture toughness.
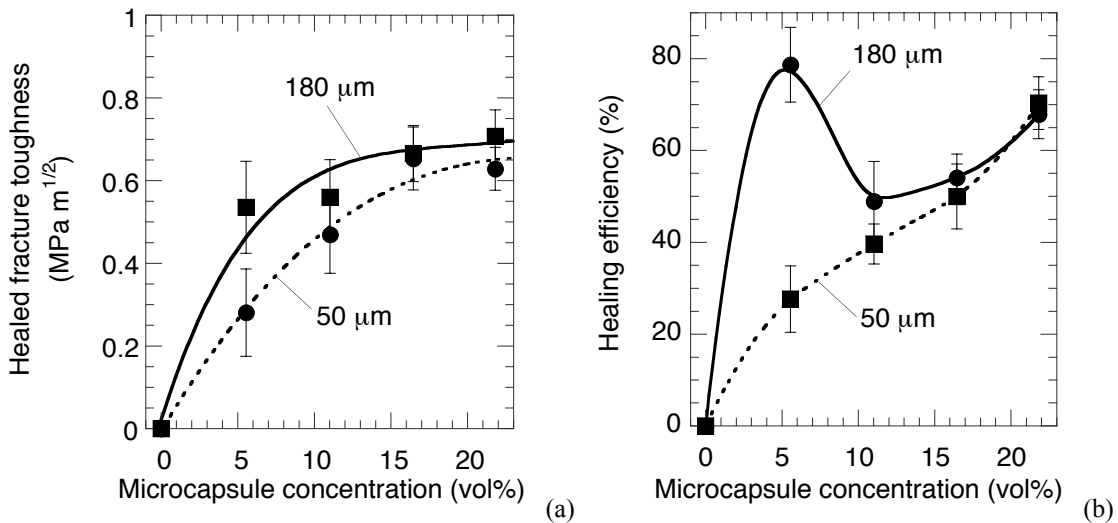

Figure 4 Influence of microcapsule concentration on self-healing behavior. (a) Healed fracture toughness and (b) healing efficiency as a function of concentration for 50 μm and 180 μm diameter microcapsules.

vol% for both cases. The healing efficiency (Fig. 4b) calculated via Eq. (2) depends more significantly on capsule diameter. The maximum healing efficiency for 180 μm microcapsules occurs at low concentrations (~5 vol%) just prior to the peak virgin fracture toughness (Fig. 3). For 50 μm microcapsules, high healing efficiency only occurs at higher microcapsule concentrations (~20 vol%) since more capsules are

required to deliver the same volume of DCPD healing agent to the fracture plane. In both cases, over 70% recovery of virgin fracture toughness is obtained through careful selection of microcapsule concentration.

4. Fracture toughness comparisons

For the range of sizes and concentrations investigated, samples with embedded microcapsules have consistently higher fracture toughness than neat epoxy. Similar, but not nearly as significant toughening has been measured for particulate fillers such as solid silica microspheres [e.g. 17,18]. The microcapsules in this study consist of a thin 190 ± 30 nm shell wall surrounding a liquid core, yet their behavior *in situ* is more reflective of solid particles than voids. Previous investigations of polymers with voids report a reduction in fracture toughness with increasing void concentration [7]. In this section, the fracture behavior of epoxy with embedded microcapsules is compared to the same epoxy incorporating solid silica microspheres, UF particles, voids, or poorly bonded microcapsules.

Fracture toughness for samples with 0 to 27 vol% of 70 ± 12 μm silica microspheres is plotted in Fig. 5. Below 10 vol%, untreated silica microspheres provide little or no increase in fracture toughness from the neat resin. Above 10 vol%, the fracture toughness increases suddenly and then grows modestly with microsphere concentration.
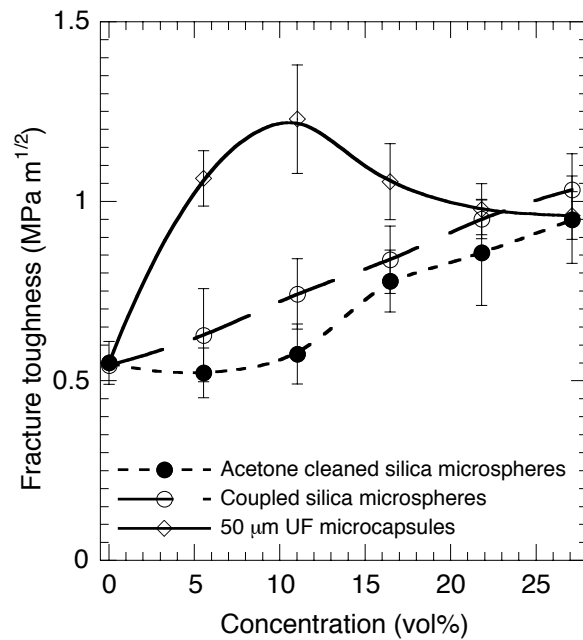

Figure 5 Fracture toughness of samples with solid silica microspheres compared to UF microcapsules as a function of concentration.

In contrast, fracture toughness increases continuously with concentration for microspheres treated with coupling agent to promote adhesion and appears to scale linearly with volume fraction. Addition of 27 vol% coupling agent treated silica microspheres yields a maximum 87% increase in toughness. In comparison, UF microcapsules induce greater toughening (127%) at a much lower concentration (11 vol%). Moreover, since silica microspheres are 2.5 times more dense than the UF microcapsules, microcapsule toughening is achieved at a greatly reduced overall weight.

The influence of embedded UF particles on fracture toughness is shown in Fig. 6. The addition of a small volume (5 vol%) of UF particles provides a 36% increase in toughness, but no further increase in toughness is observed at higher concentrations. Toughening due to the addition of solid UF particles is much less significant than toughening induced by liquid-filled UF microcapsules.

Fig. 6 illustrates the relative effects of void content and poor microcapsule bonding on epoxy fracture toughness. In both cases, toughness decreases with increasing concentrations until reaching a plateau at ~10 vol%. Microcapsules treated with release agent are easily pulled from cured epoxy and debond rather than rupture. Hence, well-bonded microcapsules induce different fracture mechanisms than voids or solid particles.
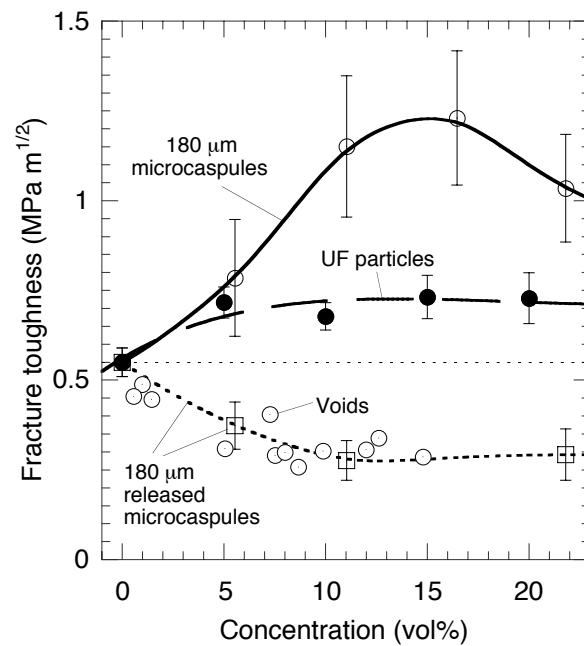

Figure 6 Comparison of fracture toughness of samples with well-bonded UF microcapsules, UF particles, voids and UF microcapsules treated with release agent.

To further clarify the operative toughening mechanisms, the fracture surfaces of the various sample types were examined by ESEM.

5. Fracture mechanisms

5.1. Neat Epoxy

Fracture surfaces of neat epoxy samples contain three distinct zones. As shown in Fig. 7a, a 37 μm thick plastic zone is present at the location of the precrack tip. The size of this region is consistent with theoretical estimates of the plastic zone using Irwin's theory [19]. The surface of the fracture plane just before the plastic zone is smooth and mirror like, typical of cleavage-like brittle fracture [20]. Immediately beyond the plastic zone, a series of hackle markings are present (Fig. 7b). Hackle marking is a feather-like fracture morphology resulting from small-scale secondary crack formation parallel to the fracture plane [20]. Within 1.5 mm of the plastic zone the hackle markings transition into striations in the direction of crack propagation (Fig. 7c). Complete transition back to a
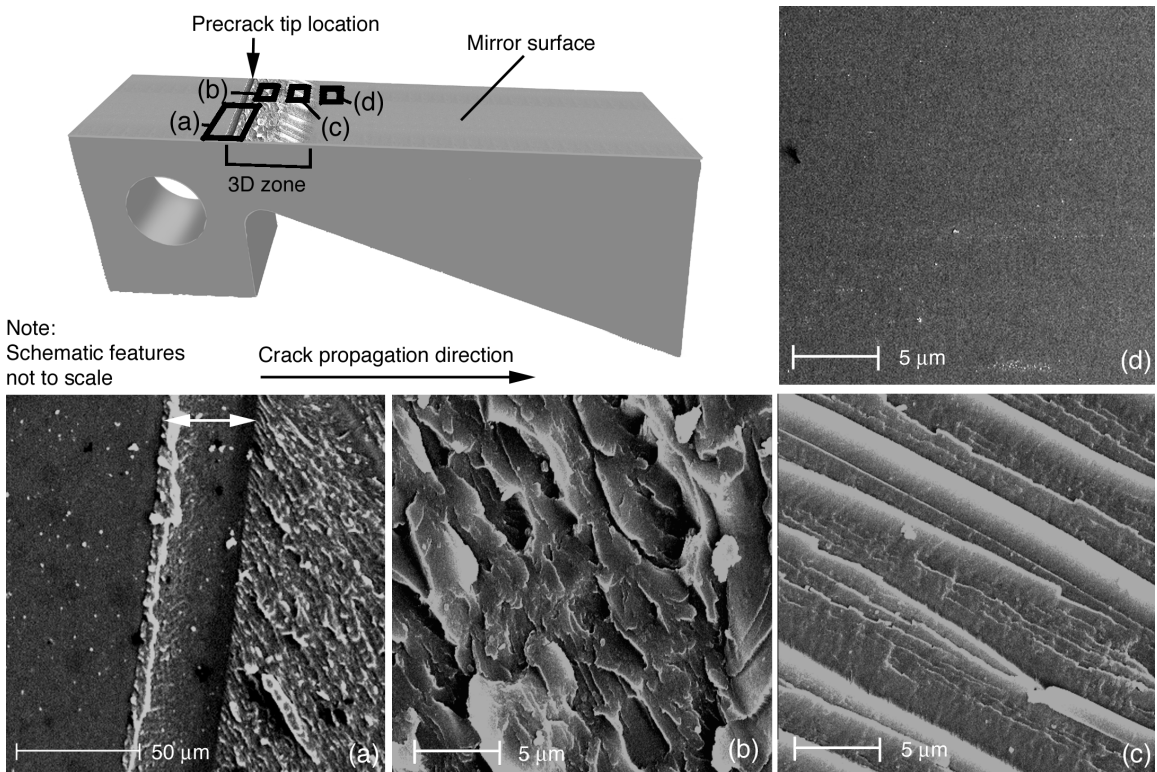
Figure 7 Electron micrographs of fracture plane in neat epoxy. (a) Precrack tip location and 37.5 μm plastic zone denoted by arrow. (b) Hackle markings following plastic zone. (c) Transition zone from hackle marking to mirror fracture surface. (d) Mirror surface of brittle fracture plane extending the length of the specimen. Note: The crack propagation is from left to right in all images

mirror fracture surface occurs within 2.0 mm as shown in Fig. 7d. The size of the hackle marking zone coincides roughly with the size of the three-dimensional (3D) stress zone (~2.2 mm) as propose by Rosakis and Ravi-Chandar [21]. Wallner lines, reported to arise from the interaction of the fracture field with associated acoustic waves [22], are present in the mirror zone of a limited number of samples.

5.2. Epoxy with embedded microcapsules

Three changes in fracture mechanism from that of neat epoxy are evident on fracture planes with embedded microcapsules. The plastic zone identified for neat epoxy is no longer present as a distinct band (Fig. 8a). Instead, there is a direct transition to hackle markings as shown in Fig. 8b. Tails originating from broken microcapsules in the fracture plane (Fig. 8c) indicate a crack pinning toughening mechanism may be operative. Crack pinning typically occurs in polymers with well-bonded, high stiffness particles, such as silica [18]. In the case of embedded microcapsules, hackle markings become the
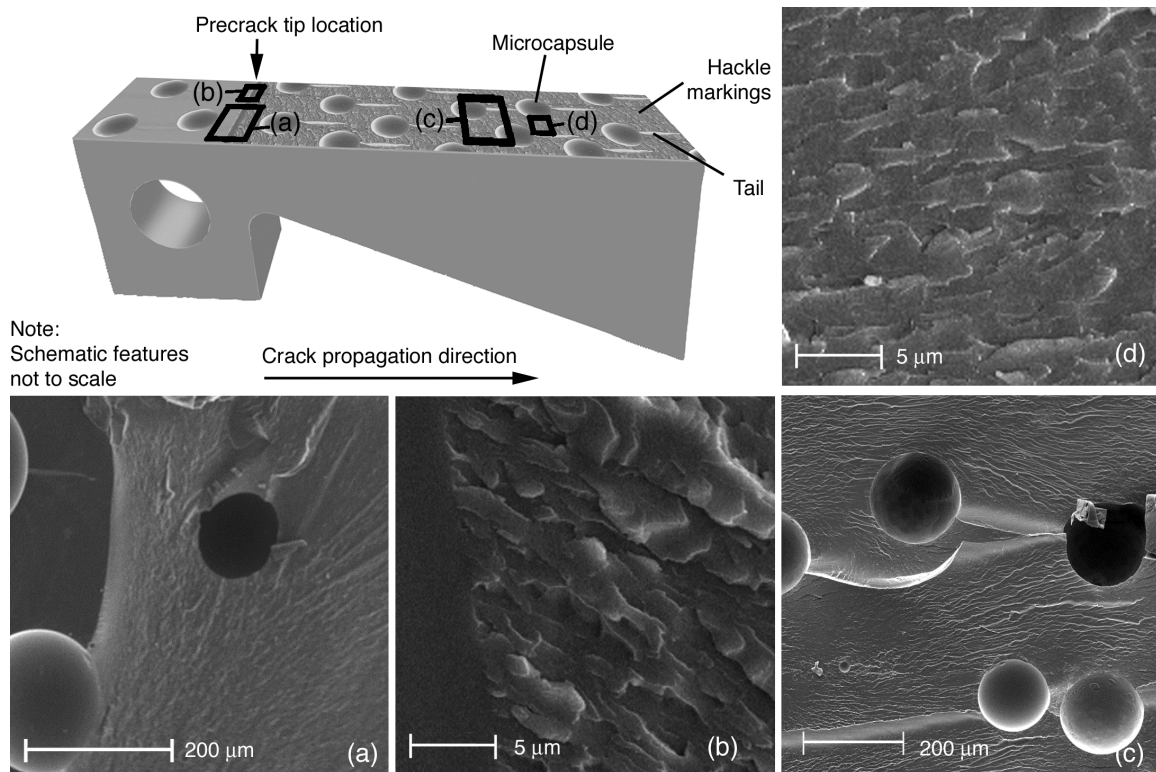
Figure 8 Electron micrographs of fracture plane in epoxy with 11 vol% 180 μm UF microcapsules. (a) Precrack tip in the presence of microcapsules lacking a defined plastic zone (b). (c) Tails in the wake of microcapsules. (d) Hackle marking presence 30 mm from precrack tip. Note: The crack propagation is from left to right in all images.

dominant fracture plane morphology. Hackle markings are present over the entire crack plane (Fig. 8d) with the degree of roughness largest near the precrack tip.

5.3. Tail structures

Tails in the wake of microcapsules form a step surface as shown in Fig. 9a. Discontinuity of the crack front in the presence of a microcapsule allows out-of-plane divergence of the crack surface on either side of the microcapsule. In order to regain continuity beyond the microcapsule, the two crack faces reconnect by formation of a step. In contrast, crack pinning by solid silica microspheres leads to the formation of a delta tail as shown in Fig. 9b. Their formation is postulated to be the result of a multistage process of crack propagation [23]. Silica microspheres first locally arrest crack growth. When sufficient energy is applied, the crack progresses along the interface of the inclusion. Tails form during snap-through when the crack front rapidly advances. The delta tail represents the lowest energy crack path. While the step tails may indicate a crack blunting process and an associated toughening mechanism, tails in the wake of microcapsules do not correspond to the classic crack pinning mechanism associated with rigid particles. Fracture planes containing UF particles contain no tails. The crack propagates through the equator of the UF particles rather than along the interface, as in the case of silica microspheres.
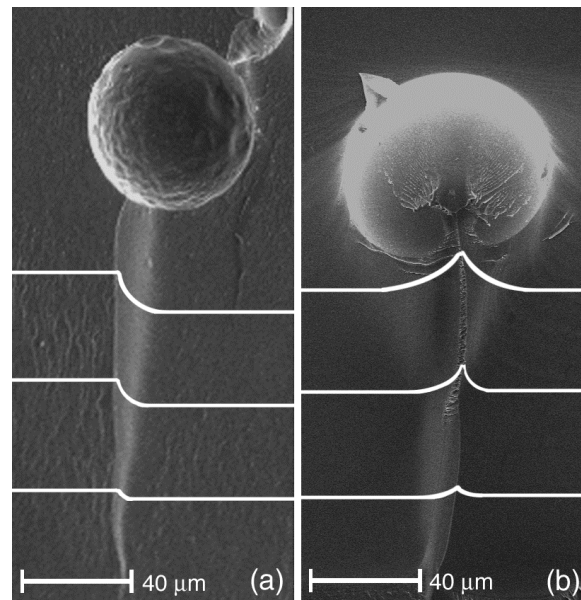

Figure 9 Electron micrographs of tail structures. (a) Step tail in wake of microcapsule and (b) delta tail in wake of silica microsphere. The crack propagation direction is from top to bottom in both images.

5.4. Hackle structure

The hackle patterns on the fracture surface of the microcapsule filled epoxy were further investigated using a cryofracture technique. The penetrating hackle structure was viewed from two perpendicular directions in the cross section, shown schematically in Fig. 10. In the view perpendicular to the crack propagation direction (Fig. 10a) finger-like extensions appear lifted from the fracture surface, indicating sub-surface damage. Cross sectional views opposite to the crack propagation direction (in Figs. 10b and 10c) reveal small cracks penetrating below the primary fracture plane. Additionally, microcracking is present beneath the fracture plane (Fig. 10d). The presence of secondary cracks in the hackle zone [24] reveal a fracture process that absorbs more elastic energy when compared to the mirror fracture surfaces of neat epoxy. The increase in the new surface area created during crack growth absorbs additional energy and increases fracture toughness.

In all the other sample types investigated other than well bonded microcapsules—neat epoxy, silica microspheres, UF particles, voids, and poorly bonded microcapsules—hackle markings were restricted to a small region near the crack tip. Fracture planes of epoxy containing voids exhibit a plastic zone, 3D zone with hackle
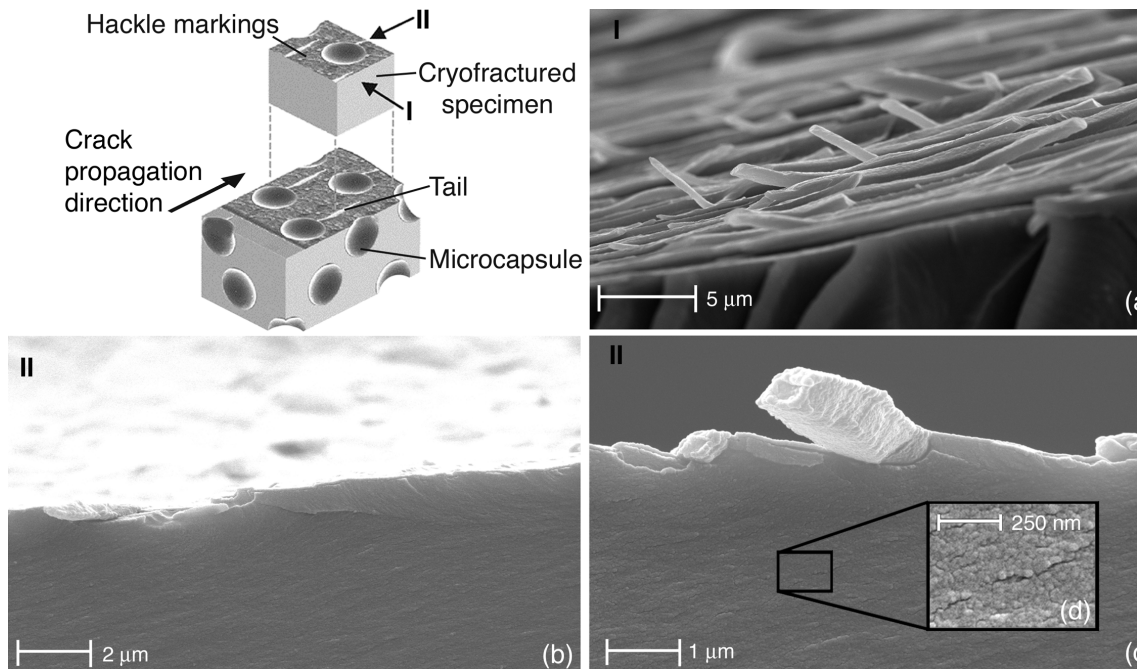

Figure 10 Electron micrographs of cryofractured specimen as viewed from (a) perpendicular to crack propagation and (b-d) opposite to the direction of crack propagation. Subsurface cracks forming hackle markings are shown in (b) and (c). Microcracks are shown in (d).

markings, and brittle mirror zone consistent with neat epoxy. In the 3D zone however, the presence of voids locally alters the fracture mechanism, causing small regions of mirror fracture surface encircling intersected voids. The resulting reduction in the total area of hackle marks may account for part of the decline in fracture toughness with the inclusion of voids.

5.5. Discussion

Although microcapsules do not behave like hard solid particles, similar fracture behavior has been observed in rubber toughened epoxy. Two separate toughening mechanisms have been identified in the literature for ductile, rubber particles: cavitation and microcracking. Embedded rubber particles respond to the imposed triaxial stress field near a crack tip by debonding from the matrix and cavitating [8, 25]. Microcapsules do not present a behavior analogous to cavitation, though polymer microcapsules ruptured by a propagating crack have been used to simulate pre-cavitated rubber particles [8]. Rubber particles also act as points of stress concentration under triaxial stress conditions generating shear yielding or microcracking in the matrix [8, 26-28]. The localized deformation and subsurface microcracking associated with rubber toughened epoxy are similar to the mechanisms identified for microcapsule toughened epoxy. The inclusion of 5 to 10 vol% of rubber particles consistently yields a 50 to 260% increase of epoxy fracture toughness [4, 8, 26-28].

6. Conclusions

Microcapsule induced toughening was investigated in a self-healing polymer composite. Both the virgin and healed fracture toughness values were strongly dependent on the size and concentration of DCPD-filled UF microcapsules added to the epoxy. Fracture toughness increased with microcapsule concentration until reaching a maximum value. The average maximum toughness was 127% greater than neat epoxy. The concentration of microcapsules at which the maximum value occurred varied with microcapsule diameter. Samples with smaller microcapsules exhibited maximum toughening at lower concentrations. Moreover, the fracture toughness measured for epoxy with embedded microcapsules was much greater than epoxy samples with similar concentrations of solid silica microspheres or UF polymer particles. Good adhesion between the microcapsules and epoxy matrix was necessary for capsule rupture and any subsequent toughening. The fracture behavior of epoxy with poor microcapsule bonding was identical to samples containing a similar concentration of voids.

Careful examination of the fracture surfaces revealed several of the operative toughening mechanisms. Fracture of the neat epoxy was brittle, exhibiting a mirror fracture surface. The addition of microcapsules produced a transition of the fracture

plane morphology to hackle markings. The increased toughening associated with fluid-filled microcapsules was attributed to increased hackle marking and subsurface microcracking not observed for solid particle fillers.

The healed fracture toughness also increased steadily with capsule concentration until reaching a plateau at about 20 vol%. The maximum healing efficiency for 180 μm diameter microcapsules occurred at low concentrations (~5 vol%) just prior to the peak virgin fracture toughness. For 50 μm microcapsules, significant healing efficiency was measured only at higher concentrations (~20 vol%). Over 70% recovery of virgin fracture toughness was achieved through careful selection of microcapsule size and concentration.

Acknowledgment

References

1. S.R. WHITE, N.R. SOTTOS, P.H. GEUBELLE, J.S. MOORE, M.R. KESSLER, S.R. SRIRAM, E.N. BROWN, and S. VISWANATHAN, *Nature* **409** (2001) 794.
2. E.L. DIAS, S.T. NGUYEN, and R.H. GRUBBS, *J. Am. Chem. Soc.* **119** (1997) 3887.
3. E.N. BROWN, N.R. SOTTOS, and S.R. WHITE, *Exp. Mech.* **42** (2002) 372.
4. H.R. AZIMI, R.A. PEARSON, and R.W. HERTZBERG, *Polym. Eng. and Sci.* **36** (1996) 2352.
5. R.J. CARDOSO, A. SHUKLA, and A. BOSE, *J. Mater. Sci.* **37** (2002) 603.
6. A.M. ZIHLIF and G. RAGOSTA, *Polym. and Polym. Compos.* **9** (2001) 345.
7. M.A. EL-HADEK and H.V. TIPPUR, *J. Mater. Sci.* **37** (2002) 1649.
8. R. BAGHERI and R.A. PEARSON, *Polymer* **37** (1996) 4529.
9. H. TODA, H. KAGAJO, K. HOSOI, T. KOBAYASHI, Y. ITO, T. HIGASHIHARA, and T. GOHDA, *J. Soc. Mater. Sci, Japan* **50** (2001) 474.
10. H.S. KIM and M.A. KHAMIS, *Compos. Part A* **32** (2001) 1311.
11. W.H. LIN and M.H.R. JEN, *J. Comp. Mater.* **32** (1998) 1356.

12. D. JUNG in "Performance and properties of embedded microspheres for self-repairing applications" (MS Thesis, University of Illinois at Urbana-Champaign, 1997) p. 105.

13. S. MOSTOVOY, P.B. CROSLEY, and E.J. RIPLING, *J. Mater*. **2** (1967) 661.

14. R.P. WOOL and K.M. O'CONNER, *J. Appl. Phys*. **52** (1981) 5953.

15. J. LEE and A.F. YEE, *Polymer* **42** (2001) 577.

16. E.N. BROWN, M.R. KESSLER, N.R. SOTTOS, and S.R. WHITE, submitted to *J. Microencapsul*. (2003).

17. J. SPANOUDAKIS and R.J. YOUNG, *J. Mater. Sci*. **19** (1984) 487.

18. P.K. MALLICK and L.J. BROUTMAN, *Mater. Sci. and Eng*. **18** (1975) 63.

19. G.R. IRWIN, in Proceedings of the 7th Sagamore Ordnance Materials Research Conference, Vol. 4, Syracuse University NY, 1960, p. 63.

20. A. RABINOVITCH, G. BELIZOVSKY, and D. BAHAT, *Phys. Rev. B* **61** (2000) 14968.

21. A.J. ROSAKIS and K. RAVI-CHANDAR, *Int. J. Solids and Struct*. **22** (1986) 121.

22. F. KERKHOF, *Glastech. Ber*. **48** (1975) 112.

23. F.F. LANGE, *Philos. Mag*. **22** (1970) 938.

24. K. RAVI-CHANDAR and W.G. KNAUSS, *Int. J. Fract*. **26** (1984) 141.

25. L. KONCZOL, W. DOLL, U. BUCHHOLZ, and R. MULHAUPT, *J. Appl. Polym. Sci*. **54** (1994) 815.

26. L. REY, N. POISSON, A. MAAZOUZ, and H. SAUTEREAU, *J. Mater. Sci*. **34** (1999) 1775.

27. J. KARGER-KOCSIS and K. FRIEDRICH, *Comp. Sci. and Technol*. **48** (1993) 263.

28. H.R. AZIMI, R.A. PEARSON, and R.W. HERTZBERG, *J. Mater. Sci*. **31** (1996) 3777.

List of Recent TAM Reports

No.	Authors	Title	Date
952	Chaïeb, S., E. Sato-Matsuo, and T. Tanaka	Shrinking-induced instabilities in gels	July 2000
953	Riahi, D. N., and A. T. Hsui	A theoretical investigation of high Rayleigh number convection in a nonuniform gravitational field—*International Journal of Pure and Applied Mathematics*, in press (2003)	Aug. 2000
954	Riahi, D. N.	Effects of centrifugal and Coriolis forces on a hydromagnetic chimney convection in a mushy layer—*Journal of Crystal Growth* **226**, 393–405 (2001)	Aug. 2000
955	Fried, E.	An elementary molecular-statistical basis for the Mooney and Rivlin–Saunders theories of rubber-elasticity—*Journal of the Mechanics and Physics of Solids* **50**, 571–582 (2002)	Sept. 2000
956	Phillips, W. R. C.	On an instability to Langmuir circulations and the role of Prandtl and Richardson numbers—*Journal of Fluid Mechanics* **442**, 335–358 (2001)	Sept. 2000
957	Chaïeb, S., and J. Sutin	Growth of myelin figures made of water soluble surfactant—Proceedings of the 1st Annual International IEEE–EMBS Conference on Microtechnologies in Medicine and Biology (October 2000, Lyon, France), 345–348	Oct. 2000
958	Christensen, K. T., and R. J. Adrian	Statistical evidence of hairpin vortex packets in wall turbulence—*Journal of Fluid Mechanics* **431**, 433–443 (2001)	Oct. 2000
959	Kuznetsov, I. R., and D. S. Stewart	Modeling the thermal expansion boundary layer during the combustion of energetic materials—*Combustion and Flame*, in press (2001)	Oct. 2000
960	Zhang, S., K. J. Hsia, and A. J. Pearlstein	Potential flow model of cavitation-induced interfacial fracture in a confined ductile layer—*Journal of the Mechanics and Physics of Solids*, **50**, 549–569 (2002)	Nov. 2000
961	Sharp, K. V., R. J. Adrian, J. G. Santiago, and J. I. Molho	Liquid flows in microchannels—Chapter 6 of *CRC Handbook of MEMS* (M. Gad-el-Hak, ed.) (2001)	Nov. 2000
962	Harris, J. G.	Rayleigh wave propagation in curved waveguides—*Wave Motion* **36**, 425–441 (2002)	Jan. 2001
963	Dong, F., A. T. Hsui, and D. N. Riahi	A stability analysis and some numerical computations for thermal convection with a variable buoyancy factor—*Journal of Theoretical and Applied Mechanics* **2**, 19–46 (2002)	Jan. 2001
964	Phillips, W. R. C.	Langmuir circulations beneath growing or decaying surface waves—*Journal of Fluid Mechanics* (submitted)	Jan. 2001
965	Bdzil, J. B., D. S. Stewart, and T. L. Jackson	Program burn algorithms based on detonation shock dynamics—*Journal of Computational Physics* (submitted)	Jan. 2001
966	Bagchi, P., and S. Balachandar	Linearly varying ambient flow past a sphere at finite Reynolds number: Part 2—Equation of motion—*Journal of Fluid Mechanics* (submitted)	Feb. 2001
967	Cermelli, P., and E. Fried	The evolution equation for a disclination in a nematic fluid—*Proceedings of the Royal Society A* **458**, 1–20 (2002)	Apr. 2001
968	Riahi, D. N.	Effects of rotation on convection in a porous layer during alloy solidification—Chapter 12 in *Transport Phenomena in Porous Media* (D. B. Ingham and I. Pop, eds.), 316–340 (2002)	Apr. 2001
969	Damljanovic, V., and R. L. Weaver	Elastic waves in cylindrical waveguides of arbitrary cross section—*Journal of Sound and Vibration* (submitted)	May 2001
970	Gioia, G., and A. M. Cuitiño	Two-phase densification of cohesive granular aggregates—*Physical Review Letters* **88**, 204302 (2002) (in extended form and with added co-authors S. Zheng and T. Uribe)	May 2001
971	Subramanian, S. J., and P. Sofronis	Calculation of a constitutive potential for isostatic powder compaction—*International Journal of Mechanical Sciences* (submitted)	June 2001

No.	Authors	Title	Date
972	Sofronis, P., and I. M. Robertson	Atomistic scale experimental observations and micromechanical/continuum models for the effect of hydrogen on the mechanical behavior of metals—*Philosophical Magazine* (submitted)	June 2001
973	Pushkin, D. O., and H. Aref	Self-similarity theory of stationary coagulation—*Physics of Fluids* **14**, 694–703 (2002)	July 2001
974	Lian, L., and N. R. Sottos	Stress effects in ferroelectric thin films—*Journal of the Mechanics and Physics of Solids* (submitted)	Aug. 2001
975	Fried, E., and R. E. Todres	Prediction of disclinations in nematic elastomers—*Proceedings of the National Academy of Sciences* **98**, 14773–14777 (2001)	Aug. 2001
976	Fried, E., and V. A. Korchagin	Striping of nematic elastomers—*International Journal of Solids and Structures* **39**, 3451–3467 (2002)	Aug. 2001
977	Riahi, D. N.	On nonlinear convection in mushy layers: Part I. Oscillatory modes of convection—*Journal of Fluid Mechanics* **467**, 331–359 (2002)	Sept. 2001
978	Sofronis, P., I. M. Robertson, Y. Liang, D. F. Teter, and N. Aravas	Recent advances in the study of hydrogen embrittlement at the University of Illinois—Invited paper, Hydrogen–Corrosion Deformation Interactions (Sept. 16–21, 2001, Jackson Lake Lodge, Wyo.)	Sept. 2001
979	Fried, E., M. E. Gurtin, and K. Hutter	A void-based description of compaction and segregation in flowing granular materials—*Proceedings of the Royal Society of London A* (submitted)	Sept. 2001
980	Adrian, R. J., S. Balachandar, and Z.-C. Liu	Spanwise growth of vortex structure in wall turbulence—*Korean Society of Mechanical Engineers International Journal* **15**, 1741–1749 (2001)	Sept. 2001
981	Adrian, R. J.	Information and the study of turbulence and complex flow—*Japanese Society of Mechanical Engineers Journal B*, in press (2002)	Oct. 2001
982	Adrian, R. J., and Z.-C. Liu	Observation of vortex packets in direct numerical simulation of fully turbulent channel flow—*Journal of Visualization*, in press (2002)	Oct. 2001
983	Fried, E., and R. E. Todres	Disclinated states in nematic elastomers—*Journal of the Mechanics and Physics of Solids* **50**, 2691–2716 (2002)	Oct. 2001
984	Stewart, D. S.	Towards the miniaturization of explosive technology—Proceedings of the 23rd International Conference on Shock Waves (2001)	Oct. 2001
985	Kasimov, A. R., and Stewart, D. S.	Spinning instability of gaseous detonations—*Journal of Fluid Mechanics* (submitted)	Oct. 2001
986	Brown, E. N., N. R. Sottos, and S. R. White	Fracture testing of a self-healing polymer composite—*Experimental Mechanics* (submitted)	Nov. 2001
987	Phillips, W. R. C.	Langmuir circulations—*Surface Waves* (J. C. R. Hunt and S. Sajjadi, eds.), in press (2002)	Nov. 2001
988	Gioia, G., and F. A. Bombardelli	Scaling and similarity in rough channel flows—*Physical Review Letters* **88**, 014501 (2002)	Nov. 2001
989	Riahi, D. N.	On stationary and oscillatory modes of flow instabilities in a rotating porous layer during alloy solidification—*Journal of Porous Media*, in press (2002)	Nov. 2001
990	Okhuysen, B. S., and D. N. Riahi	Effect of Coriolis force on instabilities of liquid and mushy regions during alloy solidification—*Physics of Fluids* (submitted)	Dec. 2001
991	Christensen, K. T., and R. J. Adrian	Measurement of instantaneous Eulerian acceleration fields by particle-image accelerometry: Method and accuracy—*Experimental Fluids* (submitted)	Dec. 2001
992	Liu, M., and K. J. Hsia	Interfacial cracks between piezoelectric and elastic materials under in-plane electric loading—*Journal of the Mechanics and Physics of Solids*, in press (2002)	Dec. 2001
993	Panat, R. P., S. Zhang, and K. J. Hsia	Bond coat surface rumpling in thermal barrier coatings—*Acta Materialia* **51**, 239–249 (2003)	Jan. 2002
994	Aref, H.	A transformation of the point vortex equations—*Physics of Fluids* **14**, 2395–2401 (2002)	Jan. 2002

List of Recent TAM Reports (cont'd)

No.	Authors	Title	Date
995	Saif, M. T. A, S. Zhang, A. Haque, and K. J. Hsia	Effect of native Al_2O_3 on the elastic response of nanoscale aluminum films — *Acta Materialia* **50**, 2779–2786 (2002)	Jan. 2002
996	Fried, E., and M. E. Gurtin	A nonequilibrium theory of epitaxial growth that accounts for surface stress and surface diffusion — *Journal of the Mechanics and Physics of Solids*, in press (2002)	Jan. 2002
997	Aref, H.	The development of chaotic advection — *Physics of Fluids* **14**, 1315–1325 (2002); see also *Virtual Journal of Nanoscale Science and Technology*, 11 March 2002	Jan. 2002
998	Christensen, K. T., and R. J. Adrian	The velocity and acceleration signatures of small-scale vortices in turbulent channel flow — *Journal of Turbulence*, in press (2002)	Jan. 2002
999	Riahi, D. N.	Flow instabilities in a horizontal dendrite layer rotating about an inclined axis — *Proceedings of the Royal Society of London A* (submitted)	Feb. 2002
1000	Kessler, M. R., and S. R. White	Cure kinetics of ring-opening metathesis polymerization of dicyclopentadiene — *Journal of Polymer Science A* **40**, 2373–2383 (2002)	Feb. 2002
1001	Dolbow, J. E., E. Fried, and A. Q. Shen	Point defects in nematic gels: The case for hedgehogs — *Proceedings of the National Academy of Sciences* (submitted)	Feb. 2002
1002	Riahi, D. N.	Nonlinear steady convection in rotating mushy layers — *Journal of Fluid Mechanics*, in press (2003)	Mar. 2002
1003	Carlson, D. E., E. Fried, and S. Sellers	The totality of soft-states in a neo-classical nematic elastomer — *Proceedings of the Royal Society A* (submitted)	Mar. 2002
1004	Fried, E., and R. E. Todres	Normal-stress differences and the detection of disclinations in nematic elastomers — *Journal of Polymer Science B: Polymer Physics* **40**, 2098–2106 (2002)	June 2002
1005	Fried, E., and B. C. Roy	Gravity-induced segregation of cohesionless granular mixtures — *Lecture Notes in Mechanics*, in press (2002)	July 2002
1006	Tomkins, C. D., and R. J. Adrian	Spanwise structure and scale growth in turbulent boundary layers — *Journal of Fluid Mechanics* (submitted)	Aug. 2002
1007	Riahi, D. N.	On nonlinear convection in mushy layers: Part 2. Mixed oscillatory and stationary modes of convection — *Journal of Fluid Mechanics* (submitted)	Sept. 2002
1008	Aref, H., P. K. Newton, M. A. Stremler, T. Tokieda, and D. L. Vainchtein	Vortex crystals — *Advances in Applied Mathematics* **39**, in press (2002)	Oct. 2002
1009	Bagchi, P., and S. Balachandar	Effect of turbulence on the drag and lift of a particle — *Physics of Fluids* (submitted)	Oct. 2002
1010	Zhang, S., R. Panat, and K. J. Hsia	Influence of surface morphology on the adhesive strength of aluminum/epoxy interfaces — *Journal of Adhesion Science and Technology* (submitted)	Oct. 2002
1011	Carlson, D. E., E. Fried, and D. A. Tortorelli	On internal constraints in continuum mechanics — *Journal of Elasticity* (submitted)	Oct. 2002
1012	Boyland, P. L., M. A. Stremler, and H. Aref	Topological fluid mechanics of point vortex motions — *Physica D* **175**, 69–95 (2002)	Oct. 2002
1013	Bhattacharjee, P., and D. N. Riahi	Computational studies of the effect of rotation on convection during protein crystallization — *Journal of Crystal Growth* (submitted)	Feb. 2003
1014	Brown, E. N., M. R. Kessler, N. R. Sottos, and S. R. White	*In situ* poly(urea-formaldehyde) microencapsulation of dicyclopentadiene — *Journal of Microencapsulation* (submitted)	Feb. 2003
1015	Brown, E. N., S. R. White, and N. R. Sottos	Microcapsule induced toughening in a self-healing polymer composite — *Journal of Materials Science* (submitted)	Feb. 2003